

1 [Applied Clay Science](#)

2 [Volume 146](#), 15 September 2017, Pages 50–55

3 <https://doi.org/10.1016/j.clay.2017.05.007>

4 <http://www.sciencedirect.com/science/article/pii/S0169131717>

5 [30203X](#)

6  
7 DETERMINATION OF THE SPECIFIC SURFACE AREA OF LAYERED  
8 SILICATES BY METHYLENE BLUE ADSORPTION: THE ROLE OF  
9 STRUCTURE, pH AND LAYER CHARGE

10  
11  
12 Nóra Hegyesi<sup>1,2\*</sup>, Richárd T. Vad<sup>1,2</sup>, Béla Pukánszky<sup>1,2</sup>

13  
14 <sup>1</sup>Institute of Materials and Environmental Chemistry, Research  
15 Centre for Natural Sciences, Hungarian Academy of Sciences,  
16 H-1519 Budapest, P.O. Box 286, Hungary

17 <sup>2</sup>Laboratory of Plastics and Rubber Technology, Department of  
18 Physical Chemistry and Materials Science, Budapest University  
19 of Technology and Economics, H-1521 Budapest, P.O. Box 91,  
20 Hungary

21  
22  
23 \*Corresponding author: Tel: 36-1-463-2967, Fax: 36-1-463-  
24 3474, E-mail: [hegyesi.nora@mail.bme.hu](mailto:hegyesi.nora@mail.bme.hu)

25 ABSTRACT

26           The specific surface area of three layered silicates was  
27 determined by three independent methods; it was estimated from  
28 the average dimensions of individual silicate layers,  
29 determined by nitrogen adsorption using the BET model and  
30 calculated from the adsorption of methylene blue on their  
31 surface in aqueous sol. The BET model gave smaller surface  
32 areas than expected, because nitrogen molecules cannot  
33 penetrate freely into the interlayer space of the silicates.  
34 Geometric calculations and the methylene blue approach yielded  
35 very similar values for two different types of Laponite when  
36 the pH of the dispersion was adjusted to 6.5 or the edges of  
37 the silicate were modified with tetrasodium pyrophosphate  
38 dispersing agent. The measurement of surface area in water  
39 without the control of pH yielded smaller surface area,  
40 because methylene blue decreased the pH of the solution  
41 resulting in the competitive adsorption of methylene blue  
42 cations and protons at the basal surface. The methylene blue  
43 approach resulted in larger surface area than expected for the  
44 silicate with large ion exchange capacity, because of the  
45 tilted orientation of the adsorbed methylene blue molecules.  
46 All these factors must be considered during the use of the  
47 methylene blue method for the determination of the specific  
48 surface area of smectites.

49

50 KEYWORDS: methylene blue adsorption, specific surface area,  
51 Langmuir isotherm, surface orientation, pH, adsorption  
52 mechanism

53

## 54 1. INTRODUCTION

55 Methylene blue (MB) is routinely used for the  
56 determination of the specific surface area of materials in  
57 aqueous medium (Cenens and Schoonheydt, 1988; Gürses et al.,  
58 2004; Kipling and Wilson, 1960; Ruiz-Hitzky, 2001; Schoonheydt  
59 and Heughebaert, 1992). The planar molecule has a rectangular  
60 shape with the area of approximately 1.7 nm x 0.76 nm and a  
61 thickness of 0.325 nm (Ruiz-Hitzky, 2001), thus one molecule  
62 covers 1.30 nm<sup>2</sup> area (Santamarina et al., 2002). Methylene  
63 blue can interact with the surface of layered silicates both  
64 through ionic and secondary, van der Waals forces, since in  
65 water MB dissociates into a cation with one positive charge  
66 (MB<sup>+</sup>) and an anion (chloride) (see **Fig. 1**). The specific  
67 surface area and cation exchange capacity (CEC) of smectites  
68 are often determined simultaneously by the adsorption of MB  
69 on their surface (Hang and Brindley, 1970; Kahr and Madsen,  
70 1995; Yener et al., 2012). The isotherm obtained can be divided  
71 into two sections in which different interactions dominate.  
72 Below the optimum flocculation point (OFP) mainly ionic  
73 interactions develop between the silicate surface and  
74 methylene blue. Above this concentration the permanent

75 negative charges of the silicate are neutralized by MB cations  
76 thus adsorption occurs mainly by physisorption (Kahr and  
77 Madsen, 1995). In the case of smectites, the amount of MB  
78 necessary to reach the optimum flocculation point is regarded  
79 as their cation exchange capacity (Hang and Brindley, 1970)  
80 and below this point methylene blue is irreversibly bonded to  
81 the surface (Bergmann and O'Konski, 1963). In the second part  
82 of the isotherm, the adsorption of MB molecules is in dynamic  
83 equilibrium. The various aspects of the adsorption of  
84 methylene blue on the surface of smectites have already been  
85 investigated in detail (Arab et al., 2015; Chang et al., 2016;  
86 Cottet et al., 2014; Gao et al., 2016). The type of the counter  
87 ion influences the extent of cation exchange, contrary to  
88 sodium ions, calcium ions cannot be completely exchanged to  
89 MB<sup>+</sup> ions resulting in smaller apparent specific surface area  
90 values (Hang and Brindley, 1970).

91 In spite of the frequent use of the methylene blue  
92 technique for the determination of the specific surface area  
93 of layered silicates, a number of factors have not been paid  
94 attention to or have not been investigated sufficiently  
95 thoroughly yet. Up to now, only a few attempts have been made  
96 to determine the influence of cation exchange capacity and  
97 layer charge on the measured specific surface areas. Yener and  
98 co-workers, for example, studied the effect of cation exchange  
99 capacity on the surface area measured, but the CEC values used

100 were quite small (smaller than 0.34 meq/g clay) (Yener et al.,  
101 2012; Gürses et al., 2006). At small ion exchange capacity  
102 methylene blue molecules orient parallel to the surface and  
103 the surface area determined is proportional to the number of  
104 adsorbed molecules.

105 On the other hand, large layer charge was shown to lead  
106 to the tilted orientation of surfactants used for the  
107 modification of the clay (Lagaly and Weiss, 1970) with  
108 increasing tilting angles at larger surface coverages (Pozsgay  
109 et al., 2004). Sponza et al. (Sponza et al., 2015), for  
110 example, measured very large, 1295 m<sup>2</sup>/g, specific surface area,  
111 but they did not characterize their silicate sufficiently  
112 (cation exchange capacity and the size of the platelets are  
113 missing) and the authors did not give any explanation for the  
114 unrealistically large value. Tilting may occur also during the  
115 adsorption of methylene blue, but sufficient attention has not  
116 been paid to the structure of the adsorbed layer including its  
117 effect on the adsorbed amount from which the specific surface  
118 area of the silicate is derived. Moreover, large layer charge  
119 leads to the aggregation of MB molecules, but its effect on  
120 the surface area measured has not been studied either (Bujdák  
121 and Komadel, 1997; Gessner et al., 1994; Neumann et al., 2002;  
122 Pentrák et al., 2012), and especially not at adsorption levels  
123 exceeding the cation exchange capacity of the silicate  
124 (Beltrán et al., 2014).

125           The pH dependent charge of the edges of the silicate may  
126 also influence adsorption by electrostatic attraction or  
127 repulsion. Since the addition of MB into an aqueous dispersion  
128 results in the decrease of pH, the edges of the silicate  
129 platelets become positively charged below a certain pH value.  
130 Positively charged edges repulse MB<sup>+</sup> cations, thus adsorption  
131 capacity decreases resulting in smaller apparent specific  
132 surface area. According to our knowledge, the effect of pH on  
133 the measured surface area of smectites has not been studied  
134 in sufficient detail yet. Although Amrhar et al. (Amrhar et  
135 al., 2015) observed the dependence of the adsorbed amount of  
136 MB on pH for illite, adsorption was very limited and the  
137 structure of the mineral differs considerably from that of the  
138 clays studied in this work.

139           The goal of our work was to study questions related to  
140 the determination of the specific surface area of smectites,  
141 which have not been explored sufficiently yet. The structure  
142 of the adsorbed methylene blue layer was studied for a smectite  
143 with large CEC value to determine the effect of the orientation  
144 of MB molecules on the surface area obtained. We investigated  
145 the effect of measurement conditions, and specifically that  
146 of pH, on the adsorption isotherm of methylene blue on various  
147 layered silicates. The influence of the edge charge of the  
148 silicate platelets on their surface area was determined in  
149 measurements carried out with and without the control of pH.

150 Smectites with small diameter were used in the experiments,  
151 for which the ratio of the surface of the edges is not  
152 negligible compared to the total surface area of the silicate  
153 (~7%). A silicate modified at the edges was also used as  
154 reference to obtain further information about the role of edge  
155 charges in MB adsorption.

156

## 157 2. MATERIALS AND METHODS

### 158 2.1. Materials

159 Sodium montmorillonite (Nanofil 116, NaMt; density  
160 ( $\rho$ ) = 2.86 g/cm<sup>3</sup>, CEC = 1.16 meq/g, diameter (d) = 240 nm,  
161 height (h) = 0.96 nm) was obtained from Rockwood Clay  
162 Additives GmbH, while Laponite XLG ( $\rho$  = 2.53 g/cm<sup>3</sup>,  
163 CEC = 0.55 meq/g, d = 25 - 30 nm, h = 0.92 nm) and Laponite  
164 XLS ( $\rho$  = 2.53 g/cm<sup>3</sup>, CEC: no data, d = 25.0 nm, h = 0.92 nm)  
165 were purchased from Byk Additives and Instruments. Laponite  
166 XLS is prepared from XLG by modification with pyrophosphate  
167 to obtain edges with negative charges in aqueous medium. All  
168 three smectites were fine powders and were used as received;  
169 they will be abbreviated as NaMt, XLG and XLS, respectively,  
170 in the further part of the paper. The chloride salt of  
171 methylene blue (MB) trihydrate (>98.5%) and sodium chloride  
172 (NaCl, analytical grade) was obtained from Sigma-Aldrich.  
173 Phosphoric acid (85 wt%) and sodium hydroxide (NaOH, a.r.)  
174 were purchased from Reanal, Hungary. De-ionized water (MilliQ

175 reagent grade, resistance larger than 18.2 MΩcm, Millipore,  
176 USA) was used for sample preparation. All experiments were  
177 done at 25 °C unless otherwise indicated.

178

## 179 **2.2. Methods**

180 The specific surface area of the silicates was determined  
181 by nitrogen adsorption using a Quantachrom Nova 2000  
182 apparatus. Samples were degassed at 200 °C in vacuum for 24  
183 hours before the measurement. The specific surface area was  
184 obtained from the Brunauer-Emmett-Teller (BET) model (Brunauer  
185 et al., 1938) using 0.162 nm<sup>2</sup> as the area occupied by one  
186 nitrogen molecule.

187 The adsorption isotherm of MB on the silicates was  
188 determined in aqueous medium. 1.2 g silicate was dispersed in  
189 100 ml MilliQ water with 10 min ultrasonication. 100 µl of the  
190 aqueous silicate sol with the concentration (*c*) of 12 g/l was  
191 diluted with 10 ml 10 mM NaCl or 10 ml phosphate buffer (10  
192 mM, pH = 6.5) to keep the ionic strength constant during the  
193 experiments. Various amounts (0-1200 µl) of aqueous MB  
194 solution (*c* = 1.95 mM) was added to the sol and the samples  
195 were stirred intensively at 25 °C for 24 h to reach  
196 equilibrium. Subsequently the dispersion was centrifuged  
197 at 13 500 rpm for 10 min and the absorbance of the supernatant  
198 was determined in a glass cuvette (path length = 1 cm) using  
199 a Unicam UV 500 UV-Vis spectrophotometer. MB concentration was



200 calculated after calibration with aqueous solutions  
201 ( $\lambda = 665 \text{ nm}$ ,  $\varepsilon = 6.24 \cdot 10^5 \text{ M}^{-1}\text{cm}^{-1}$ ). As the silicates were not  
202 dried before the adsorption measurements, water content had  
203 to be determined to obtain the amount of dry silicate. Water  
204 content was deduced from thermogravimetric analysis (TGA6,  
205 Perkin Elmer). The weight change of samples of 10-15 mg were  
206 measured in nitrogen atmosphere in the temperature range of  
207 30-800 °C with 10 °C/min heating rate. The pH of buffer  
208 solutions was checked with a pH/ion analyzer (Radelkis OP-  
209 271/1). All adsorption experiments were done in polyethylene  
210 centrifuge tubes to avoid the adsorption of MB on the surface  
211 of the container. The amount of adsorbed MB was determined by  
212 thermogravimetric analysis as well. Solid MB was added to  
213 aqueous silicate sols ( $c = 10 \text{ g/l}$ ) and left standing for 24  
214 hours. The dispersions were centrifuged, precipitates were  
215 dried at 60 °C and then characterized by TGA. Measurements  
216 were carried out in oxygen atmosphere in the temperature range  
217 of 30-800 °C with 10 °C/min heating rate (TGA6, Perkin Elmer).  
218 After MB adsorption and drying the gallery structure of the  
219 silicates was characterized by X-ray diffraction using a  
220 Philips PW 1830/PW 1050 equipment with  $\text{CuK}\alpha$  radiation  
221 (0.154 nm) at 40 kV and 35 mA anode excitation with 0.04 step  
222 size and 4 s counting time. Zeta potential was determined in  
223 the same supernatant solutions used also for the measurement  
224 of the concentration of methylene blue in the adsorption

225 experiments by using a ZetaPALS analyser (Brookhaven  
226 Instruments Co.) at 30 °C in polystyrene cuvettes. The  
227 Smoluchowski equation (**Eq. 1**) was used for the calculation of  
228 zeta potential:

$$229 \quad \xi = \frac{\mu_E \eta}{\varepsilon} \quad (1)$$

230 where  $\xi$  is zeta potential,  $\mu_E$  is electrophoretic mobility,  
231 while  $\eta$  is the viscosity and  $\varepsilon$  the permittivity of water (Wall,  
232 2002). Five parallel runs were done on each sample and each  
233 run consisted of 10 cycles.

234

### 235 3. RESULTS AND DISCUSSION

236 The results are presented in three separate sections. The  
237 adsorption isotherms of methylene blue on the various  
238 silicates is described first together with the fitting of  
239 models and the calculation of the specific surface area of the  
240 silicates. This section includes the comparison of results  
241 obtained by various methods and the interpretation of the  
242 differences observed. The effect of pH on the adsorption of  
243 methylene blue on the surface of smectites is discussed in the  
244 next section followed by considerations about the influence  
245 of charge density on the orientation of adsorbed molecules and  
246 thus on the specific surface area determined.

247

248

### 249 **3.1. Adsorption isotherms**

250           The three smectites compared have different structure and  
251 surface properties. Sodium montmorillonite (NaMt) is a  
252 dioctahedral layered silicate with aluminum partially  
253 substituted by magnesium in the octahedral sheets, while  
254 Laponites are synthetic trioctahedral smectites in which  
255 magnesium is partially substituted by lithium. Both types of  
256 silicates have negatively charged basal surfaces in aqueous  
257 medium, but the surface charge of the edges is different. NaMt  
258 and XLG have pH dependent charge at their edges (Pecini and  
259 Avena, 2013; Tawari et al., 2001; Willenbacher, 1996), while  
260 XLS is modified with tetrasodium pyrophosphate dispersing  
261 agent that results in negative charges (Brunier et al., 2016).  
262 The specific surface area of the three smectites was  
263 determined by three independent approaches. The BET model was  
264 applied for the evaluation of the results of nitrogen  
265 adsorption measurements and the specific surface area  
266 determined in this way is the BET surface ( $A_{\text{BET}}$ ). Surface area  
267 was also calculated from the dimensions of the individual  
268 platelets, from their average height (h), diameter (d) and  
269 density ( $\rho$ ) to obtain the geometric surface area ( $A_g$ ). These  
270 two values are compared to that obtained by the third method,  
271 which was the methylene blue approach ( $A_{\text{MB}}$ ).

272           The method is based on the determination of an adsorption  
273 isotherm, the fitting of models to the isotherms and the

274 calculation of the specific surface area from them. The  
275 adsorption isotherms measured on the three smectites studied  
276 is presented in **Fig. 2**. The amount of adsorbed MB converges  
277 towards an equilibrium value. The largest adsorption is  
278 measured on NaMt and smaller values for the two Laponites. The  
279 large difference between the latter two is quite surprising,  
280 since the geometry and size of the silicate platelets are the  
281 same, only the surface charge of the edges differs. The  
282 dissimilarity calls the attention to the importance of the  
283 character and behavior of the functional groups located at the  
284 edges of the platelets, but also to that of measurement  
285 conditions, including the pH of the medium used.

286       The adsorption of MB onto solid surfaces from aqueous  
287 medium is usually described with the Langmuir or the  
288 Freundlich isotherm. The Langmuir isotherm assumes an  
289 energetically homogenous surface of identical adsorption  
290 sites, definite number of these latter, monomolecular coverage  
291 and the lack of interaction among the adsorbed molecules. The  
292 model has the advantage of providing constants with physical  
293 meaning and it usually performs well when the surface is  
294 homogeneous and only one type of adsorption site exists. The  
295 model can be expressed in the following way to describe liquid-  
296 solid equilibrium quantitatively

$$297 \quad C_s = \frac{K_L S_m C_L}{1 + K_L C_L} \quad (2)$$

298 where  $C_s$  is the amount of MB adsorbed on the solid surface at  
299 equilibrium (M),  $C_L$  is the equilibrium concentration of MB  
300 (M),  $S_m$  is the apparent sorption capacity or adsorption maximum  
301 (mol/g) and  $K_L$  is the Langmuir coefficient (g/mol). **Eq. 2** can  
302 be expressed in a linear form

$$303 \quad \frac{C_L}{C_s} = \frac{1}{K_L S_m} + \frac{C_L}{S_m} \quad (3)$$

304 Plotting the results according to **Eq. 3**, i.e.  $C_L/C_s$  against  
305 the equilibrium concentration of methylene blue ( $C_L$ ) should  
306 result in a straight line from which the maximum amount of  
307 adsorbed material and the specific surface area can be  
308 determined. The linear plots of the isotherms are presented  
309 in **Fig. 3** in this way and straight lines are obtained indeed  
310 with very good determination coefficients ( $R^2$ ) indicating  
311 excellent fit. The parameters derived from the fits are  
312 compiled in **Table 1**.

313 The Freundlich model can handle energetically  
314 heterogeneous surfaces, multilayer and infinite coverage, but  
315 it lacks the proper thermodynamic basis. It can be expressed  
316 as

$$317 \quad q_e = K_F c_e^{\frac{1}{n}} \quad (4)$$

318 where  $q_e$  is the adsorbed amount of the adsorbate (mol/g),  $c_e$   
319 the equilibrium concentration of the sorbate (M),  $K_F$  (mol/g)  
320 relates to adsorption capacity (larger  $K_F$  indicates larger  
321 maximum capacity), while  $n$  gives information about surface

322 heterogeneity and the interactions between the adsorbent and  
323 adsorbate. The Freundlich isotherm can also be linearized and  
324 it takes the following form

$$325 \quad \log q_e = \log K_F + \frac{1}{n} \log c_e \quad (5)$$

326 The linear form of Freundlich model was also fitted to the  
327 experimental data and the results are shown in **Fig. 4**. The  
328 quantities determined are also collected in **Table 1**.

329 The comparison of determination coefficients ( $R^2$ )  
330 indicates that the Langmuir model describes the experimental  
331 results better than the Freundlich model. The better fit also  
332 implies that the surface of the silicates studied is  
333 energetically homogenous and a monomolecular coverage develops  
334 during adsorption. Accordingly, the maximum sorption capacity  
335 and the specific surface area of the silicates were derived  
336 from the Langmuir model. The comparison of the specific  
337 surface areas obtained by the different approaches allows the  
338 drawing of several conclusions. Surface areas resulting from  
339 the geometry of the platelets and that determined by the  
340 adsorption of methylene blue are larger than values obtained  
341 by the BET model. This is not very surprising since the  
342 penetration of nitrogen molecules into the gallery space of  
343 the dry silicate is quite limited. It is worth to note that  
344 some correlation can be seen between the penetration of  
345 nitrogen molecules and the regularity of gallery structure.

346 The X-ray diffractogram of NaMt indicates a relatively large  
347 degree of order, while regularity is much smaller for the two  
348 Laponites (**Fig 5**). Regular stacks with large diameter result  
349 in a BET surface area for NaMt one order of magnitude smaller  
350 than the geometric surface area, while the Laponite powders  
351 consist of more randomly arranged disks with small diameter.  
352 Differences can be observed also between surface areas  
353 obtained by MB adsorption and geometric calculations for NaMt  
354 and XLG. The deviations are unexpected because the MB method  
355 is widely accepted and used for the determination of the  
356 specific surface area of smectites and they obviously need  
357 further study and considerations.

358

### 359 **3.2. Competitive adsorption, the effect of pH**

360 The surface area determined by the adsorption of  
361 methylene blue on XLG is considerably smaller (654 m<sup>2</sup>/g  
362 calculated from the sorption capacity of 0.838 mmol/g clay)  
363 than its geometric surface area,  $A_g$  (922 m<sup>2</sup>/g). On the other  
364 hand, the MB surface area of XLS is significantly larger  
365 (1.175 mmol/g silicate, 917 m<sup>2</sup>/g) and equals the geometric  
366 one. Since XLS is produced from XLG by the modification of its  
367 edges, this dissimilarity in binding capacity must be caused  
368 by the influence of the tetrasodium pyrophosphate dispersing  
369 agent. XLG has Si-OH and Mg-OH groups on their edges. Si-OH  
370 groups are deprotonated above pH = 4.5-5, while for oxides and

371 hydroxides of magnesium zero charge is reached above  $\text{pH} = 10$   
372 (Kosmulski, 2016), i.e. the charge of the edges depends on  $\text{pH}$ .  
373 The dependence of MB adsorption on  $\text{pH}$  has been observed before  
374 (Amrhar et al., 2015). The  $\text{pH}$  of silicate sols decreases upon  
375 the addition of methylene blue as shown by **Fig. 6** resulting  
376 in the protonation of the edges thus repulsive interactions  
377 may develop between them and  $\text{MB}^+$  cations.

378 However, the difference between the measured specific  
379 surface area and the area of the basal surface ( $268 \text{ m}^2/\text{g}$ ) is  
380 larger than the surface area of the edges ( $63 \text{ m}^2/\text{g}$ ). As a  
381 consequence, another effect must hinder the adsorption of  $\text{MB}^+$   
382 onto the surface of XLG at small  $\text{pH}$  values. The increase in  
383 proton concentration results in the competitive adsorption of  
384  $\text{MB}^+$  cations and protons onto the basal surface of this  
385 smectite, i.e. in smaller equilibrium  $\text{MB}^+$  adsorption. In the  
386 case of XLS, the lack of competitive adsorption can be  
387 explained with the larger  $\text{pH}$  of XLS dispersions (see **Fig. 6**)  
388 and the permanent negative charge of its edges due to the  
389 modification with tetrasodium pyrophosphate.

390 The repulsive forces between XLG and  $\text{MB}^+$  were confirmed  
391 by zeta potential measurements. In **Fig. 7** zeta potential is  
392 plotted against the amount of MB added to the sol for the XLG  
393 sample suspended in distilled water or in a buffer solution  
394 at  $\text{pH} 6.5$ , and also for XLS as reference. At small amount of  
395 MB the zeta potential of the sol containing the silicate



396 particles is negative both in water and in the buffer solution.  
397 Without pH control XLG has a negative to positive transition  
398 in zeta potential as a function of the amount of MB, because  
399 of its positively charged edges. On the other hand, the zeta  
400 potential of the sol buffered to pH 6.5 containing XLG and  
401 that of the sol prepared from XLS does not take positive values  
402 independently of the added amount of MB showing that repulsive  
403 electrostatic forces do not develop among the components.

404 In order to prove the effect of pH, adsorption  
405 measurements were carried out with XLG in a buffered solution  
406 at pH = 6.5 and an adsorption isotherm was recorded. The  
407 Langmuir model was fitted to the experimental data, and the  
408 maximum amount of adsorbed MB determined at controlled pH was  
409 1.162 mmol/g silicate corresponding to a specific surface area  
410 of 906 m<sup>2</sup>/g. This value almost equals the geometric (922 m<sup>2</sup>/g)  
411 and the MB surface area of XLS (917 m<sup>2</sup>/g) that strongly  
412 corroborates our hypothesis about the competitive adsorption  
413 of MB<sup>+</sup> and H<sup>+</sup>.

414 When pH is controlled, the adsorption of MB<sup>+</sup> cations is  
415 favored on the silicate surface and they neutralize the  
416 negative charges of the surface. Instead of protonation,  
417 functional groups at the edges and the negatively charged  
418 basal surface of the silicate are covered by MB<sup>+</sup> cations  
419 resulting in zero zeta potential (Pecini and Avena, 2013). In  
420 this case, the amount of adsorbed MB is determined only by the

421 surface area of the silicate.

422

### 423 **3.3. Cation exchange capacity, orientation**

424 The other surprising result which needs explanation is  
425 the large specific surface area obtained for sodium  
426 montmorillonite by the methylene blue approach. Literature  
427 references give a value of 750 m<sup>2</sup>/g (Santamarina et al., 2002)  
428 specific surface area for this silicate and the value obtained  
429 from geometric calculations is 734 m<sup>2</sup>/g (see [Table 1](#)). However,  
430 the maximum amount of MB adsorbed by NaMt was 1.377 mmol/g  
431 that translates to a specific surface area of 1074 m<sup>2</sup>/g, which  
432 exceeds considerably both values mentioned above. The  
433 difference can be explained with the large cation exchange  
434 capacity of the NaMt used which is 1.16 meq/g. If all the  
435 charges were neutralized by MB cations, the covered surface  
436 would be 904 m<sup>2</sup>/g assuming that the adsorbed molecules are  
437 oriented parallel to the silicate platelets. The only  
438 reasonable explanation is that MB molecules are tilted to the  
439 basal surface of NaMt, or coverage is not monomolecular. The  
440 tilted orientation of adsorbed molecules (surfactants) was  
441 observed earlier on layered silicates, when CEC was  
442 sufficiently large (Lagaly and Weiss, 1970).

443 The gallery structure of the silicate samples was checked  
444 by XRD measurements and layer distance was calculated from the  
445 position of the silicate reflection observed in the recorded

446 XRD patterns. The orientation of MB molecules among the  
447 silicate layers was determined as a function of the adsorbed  
448 amount of MB. This latter was measured by TGA on centrifuged  
449 and dried silicate samples. The layer distance of all  
450 investigated silicates increased as a result of MB adsorption  
451 indicated by the shift of the silicate reflection towards  
452 smaller  $2\theta$  degrees in the diffractograms (not shown). The  
453 dependence of layer distance on the amount of adsorbed MB is  
454 presented in **Fig. 8**.

455 Tilted orientation can be confirmed by comparing the  
456 dependence of layer distance on MB content for NaMt and XLG,  
457 respectively. Layer distance increases stepwise for XLG having  
458 an ion exchange capacity of 0.55 meq/g (see **Fig. 8**). Below 0.6  
459 mmol MB/g Laponite, the layer distance indicates monolayer  
460 coverage. The thickness of one MB molecule is 0.325 nm, while  
461 that of an XLG platelet is 0.92 nm. Layer distance is 1.37 nm  
462 when the amount of adsorbed MB is less than 0.62 mmol/g, which  
463 is close to the combined thickness of the platelet and the dye  
464 molecule (1.25 nm). At larger amount of adsorbed MB, above  
465 0.62 mmol/g, the dye molecules can only be arranged in a double  
466 layer among the collapsed silicate disks. In this case, the  
467 layer distance is 1.5 nm, which is close to the sum of the  
468 thicknesses of one silicate layer and two MB molecules  
469 (1.57 nm). In the case of NaMt having large CEC, a continuous  
470 increase of layer distance is observed with increasing MB

471 content that indicates the tilted, non-parallel orientation  
472 of the adsorbed molecules among the silicate layers. In this  
473 case, dye molecules do not lie parallel to the surface of the  
474 clay and the specific surface area determined from MB  
475 adsorption is apparently larger than at monomolecular coverage  
476 and parallel orientation. Specific surface area can be  
477 calculated through geometric consideration by taking into  
478 account the tilting of the molecules. Values between 724 and  
479 803 m<sup>2</sup>/g were obtained in this way, which agree well with  
480 published data and the value determined from the geometry of  
481 silicate platelets.

482

#### 483 4. CONCLUSIONS

484 The specific surface area of three layered silicates was  
485 determined by three different approaches and good agreement  
486 was observed for some of the results, while considerable  
487 discrepancies in other cases. If adsorption occurs through  
488 attractive ionic forces and the adsorbed molecules are  
489 arranged parallel to the silicate layers in a monomolecular  
490 coverage, the agreement between surface areas calculated from  
491 the geometry of the plates and those determined by the  
492 adsorption of methylene blue agree well with each other. The  
493 specific surface area of a silicate with relatively small size  
494 (Laponite XLG) was smaller than expected because of the  
495 dependence of the adsorbed amount of MB molecules on pH. The

496 addition of methylene blue solution decreases pH considerably  
497 leading to particles with positive charge, as shown by zeta  
498 potential measurements, to smaller methylene blue adsorption  
499 and small specific surface area. Modification of the clay or  
500 the control of pH by a buffer solve the problem, and real  
501 values for surface areas are obtained which agree well with  
502 geometric calculations. At large ion exchange capacity (NaMt,  
503 CEC = 1.16 meq/g), the molecules adsorb in a tilted  
504 orientation and not parallel to the surface. Tilted  
505 orientation results in larger than monomolecular coverage and  
506 the specific surface area calculated from MB adsorption is  
507 considerably larger than the real surface of the silicate.

508

#### 509 5. ACKNOWLEDGEMENTS

510 The authors are indebted to Krisztina László and György  
511 Bosznai for their help in the nitrogen adsorption  
512 measurements. The authors acknowledge the financial support  
513 of the National Scientific Research Fund of Hungary (OTKA  
514 Grant No. K 120039). One of the authors (N. Hegyesi) thanks  
515 Pro Progressio Foundation for her scholarship.

516

#### 517 6. REFERENCES

518 Amrhar, O.; Nassali, H.; Elyoubi, M. S., Adsorption of a  
519 cationic dye, Methylene Blue, onto Moroccan Illitic Clay.

520 Journal of Materials and Environmental Science 2015, 6  
521 (11), 3054-3065.

522 Arab, P.B., Araújo, T.P., Pejon, O.J., 2015. Identification  
523 of clay minerals in mixtures subjected to differential  
524 thermal and thermogravimetry analyses and methylene blue  
525 adsorption tests. Applied Clay Science 114, 133-140.

526 Beltrán, M.I., Benavente, V., Marchante, V., Dema, H.,  
527 Marcilla, A., 2014. Characterisation of montmorillonites  
528 simultaneously modified with an organic dye and an  
529 ammonium salt at different dye/salt ratios. Properties  
530 of these modified montmorillonites EVA nanocomposites.  
531 Applied Clay Science 97-98, 43-52.

532 Bergmann, K., O'Konski, C.T., 1963. A spectroscopic study of  
533 methylene blue monomer, dimer, and complexes with  
534 montmorillonite. The Journal of Physical Chemistry 67,  
535 2169-2177.

536 Brunauer, S., Emmett, P.H., Teller, E., 1938. Adsorption of  
537 Gases in Multimolecular Layers. Journal of the American  
538 Chemical Society 60, 309-319.

539 Brunier, B., Sheibat-Othman, N., Chniguir, M., Chevalier, Y.,  
540 Bourgeat-Lami, E., 2016. Investigation of Four Different  
541 Laponite Clays as Stabilizers in Pickering Emulsion  
542 Polymerization. Langmuir 32, 6046-6057.

543 Bujdák, J., Komadel, P., 1997. Interaction of Methylene Blue  
544 with Reduced Charge Montmorillonite. The Journal of  
545 Physical Chemistry B 101, 9065-9068.

546 Cenens, J., Schoonheydt, R.A., 1988. Visible spectroscopy of  
547 methylene blue on hectorite, laponite B, and barasym in  
548 aqueous suspension. Clays and Clay Minerals 36, 214-224.

549 Chang, J., Ma, J., Ma, Q., Zhang, D., Qiao, N., Hu, M., Ma,  
550 H., 2016. Adsorption of methylene blue onto  
551 Fe<sub>3</sub>O<sub>4</sub>/activated montmorillonite nanocomposite. Applied  
552 Clay Science 119, Part 1, 132-140.

553 Cottet, L., Almeida, C.A.P., Naidek, N., Viante, M.F., Lopes,  
554 M.C., Debacher, N.A., 2014. Adsorption characteristics  
555 of montmorillonite clay modified with iron oxide with  
556 respect to methylene blue in aqueous media. Applied Clay  
557 Science 95, 25-31.

558 Gao, W., Zhao, S., Wu, H., Deligeer, W., Asuha, S., 2016.  
559 Direct acid activation of kaolinite and its effects on  
560 the adsorption of methylene blue. Applied Clay Science  
561 126, 98-106.

562 Gessner, F., Schmitt, C.C., Neumann, M.G., 1994. Time-  
563 Dependent Spectrophotometric Study of the Interaction of  
564 Basic Dyes with Clays. I. Methylene Blue and Neutral Red  
565 on Montmorillonite and Hectorite. Langmuir 10, 3749-3753.

566 Gürses, A.; Doğar, Ç.; Yalçın, M.; Açıkıldız, M.; Bayrak, R.;  
567 Karaca, S., The adsorption kinetics of the cationic dye,

568 methylene blue, onto clay. Journal of Hazardous Materials  
569 2006, 131 (1-3), 217-228.

570 Gürses, A., Karaca, S., Doğar, Ç., Bayrak, R., Açıkıldız, M.,  
571 Yalçın, M., 2004. Determination of adsorptive properties  
572 of clay/water system: methylene blue sorption. Journal  
573 of Colloid and Interface Science 269, 310-314.

574 Hang, P.T., Brindley, G.W., 1970. Methylene Blue Absorption  
575 by Clay Minerals. Determination of Surface Areas and  
576 Cation Exchange Capacities (Clay-Organic Studies XVIII).  
577 Clays and Clay Minerals 18, 203-212.

578 Kahr, G., Madsen, F.T., 1995. Determination of the cation  
579 exchange capacity and the surface area of bentonite,  
580 illite and kaolinite by methylene blue adsorption.  
581 Applied Clay Science 9, 327-336.

582 Kipling, J.J., Wilson, R.B., 1960. Adsorption of methylene  
583 blue in the determination of surface areas. Journal of  
584 Applied Chemistry 10, 109-113.

585 Kosmulski, M., 2016. Isoelectric points and points of zero  
586 charge of metal (hydr)oxides: 50 years after Parks'  
587 review. Advances in Colloid and Interface Science 238,  
588 1-61.

589 Lagaly, G., Weiss, A., 1970. Anordnung und Orientierung  
590 kationischer Tenside auf ebenen Silicatoberflächen. I.  
591 Darstellung der n-Alkylammoniumderivate von



592 glimmerartigen Schichtsilicaten. Kolloid-Zeitschrift und  
593 Zeitschrift für Polymere 237, 266-273.

594 Neumann, M.G., Gessner, F., Schmitt, C.C., Sartori, R., 2002.  
595 Influence of the Layer Charge and Clay Particle Size on  
596 the Interactions between the Cationic Dye Methylene Blue  
597 and Clays in an Aqueous Suspension. Journal of Colloid  
598 and Interface Science 255, 254-259.

599 Pecini, E.M., Avena, M.J., 2013. Measuring the Isoelectric  
600 Point of the Edges of Clay Mineral Particles: The Case  
601 of Montmorillonite. Langmuir 29, 14926-14934.

602 Pentrák, M., Czímerová, A., Madejová, J., Komadel, P., 2012.  
603 Changes in layer charge of clay minerals upon acid  
604 treatment as obtained from their interactions with  
605 methylene blue. Applied Clay Science 55, 100-107.

606 Pozsgay, A., Fráter, T., Százdí, L., Müller, P., Sajó, I.,  
607 Pukánszky, B., 2004. Gallery structure and exfoliation  
608 of organophilized montmorillonite: effect on composite  
609 properties. European Polymer Journal 40, 27-36.

610 Ruiz-Hitzky, E., 2001. Molecular access to intracrystalline  
611 tunnels of sepiolite. Journal of Materials Chemistry 11,  
612 86-91.

613 Santamarina, J.C., Klein, K.A., Wang, Y.H., Prencke, E., 2002.  
614 Specific surface: determination and relevance. Canadian  
615 Geotechnical Journal 39, 233-241.

616 Schoonheydt, R.A., Heughebaert, L., 1992. Clay adsorbed dyes  
617 - methylene blue on Laponite. *Clay Minerals*. 27, 91-100.  
618 Sponza, A.; Fernandez, N.; Yang, D.; Ortiz, K.; Navarro, A.,  
619 Comparative Sorption of Methylene Blue onto Hydrophobic  
620 Clays. *Environments* 2015, 2 (3), 388-398.  
621 Tawari, S.L., Koch, D.L., Cohen, C., 2001. Electrical Double-  
622 Layer Effects on the Brownian Diffusivity and Aggregation  
623 Rate of Laponite Clay Particles. *Journal of Colloid and*  
624 *Interface Science* 240, 54-66.  
625 Wall, S., 2002. Solid Dispersions, in: Holmberg, K. (Ed.),  
626 Handbook of Applied Surface and Colloid Chemistry. John  
627 Wiley & Sons, Ltd, West Sussex, England, pp. 3-21.  
628 Willenbacher, N., 1996. Unusual Thixotropic Properties of  
629 Aqueous Dispersions of Laponite RD. *Journal of Colloid*  
630 *and Interface Science* 182, 501-510.  
631 Yener, N., Biçer, C., Önal, M., Sarıkaya, Y., 2012.  
632 Simultaneous determination of cation exchange capacity  
633 and surface area of acid activated bentonite powders by  
634 methylene blue sorption. *Applied Surface Science* 258,  
635 2534-2539.

636

637

638

639

640

641

642

643

644

645

646

647

648

649

650

651

652

653 CAPTIONS

654 Fig. 1 The chemical structure of methylene blue.

655 Fig. 2 Adsorption isotherm of methylene blue on the surface  
656 of the investigated silicates. Symbols: ( $\Delta$ ) NaMt,  
657 ( $\circ$ ) Laponite XLS, ( $\square$ ) Laponite XLG.

658 Fig. 3 Fitting of the Langmuir model onto the adsorption  
659 isotherms of **Fig. 1**. Symbols: ( $\Delta$ ) NaMt, ( $\circ$ ) Laponite  
660 XLS, ( $\square$ ) Laponite XLG.

661 Fig. 4 Correlations obtained by the fitting of the  
662 Freundlich model to the isotherms presented in **Fig.**  
663 **1**. Symbols: ( $\Delta$ ) NaMt, ( $\circ$ ) Laponite XLS, ( $\square$ ) Laponite  
664 XLG.

665 Fig. 5 X-ray diffractograms of Laponite XLG (black), XLS

666 (red) and NaMt (blue).

667 Fig. 6 The pH of the silicate sols plotted against the added  
668 amount of methylene blue in water. Symbols: ( $\Delta$ ) NaMt,  
669 ( $\circ$ ) Laponite XLS, ( $\square$ ) Laponite XLG.

670 Fig. 7 Zeta potential of the silicate particles plotted as  
671 a function of the added amount of MB. Symbols:  
672 Laponite XLG with ( $\nabla$ ) and without ( $\square$ ) pH control,  
673 Laponite XLS ( $\circ$ ) shown as reference.

674 Fig. 8 Layer distance of silicates plotted against the  
675 amount of adsorbed methylene blue. Symbols: ( $\Delta$ ) NaMt,  
676 ( $\square$ ) Laponite XLG.

677

678 Hegyesi, Fig. 1

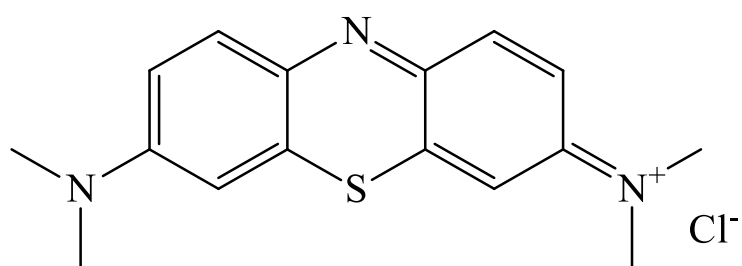
679

680

681

682

683



684

685

686

687

688

689

690

691

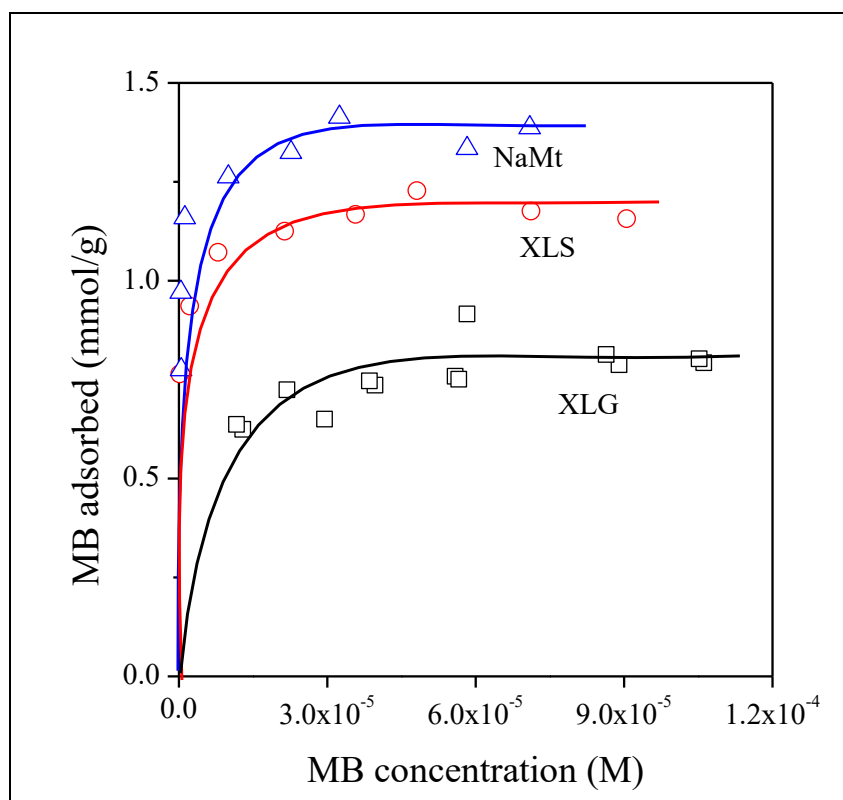
692

693

694 Hegyesi, Fig. 2

695

696



697

698

699

700

701

702

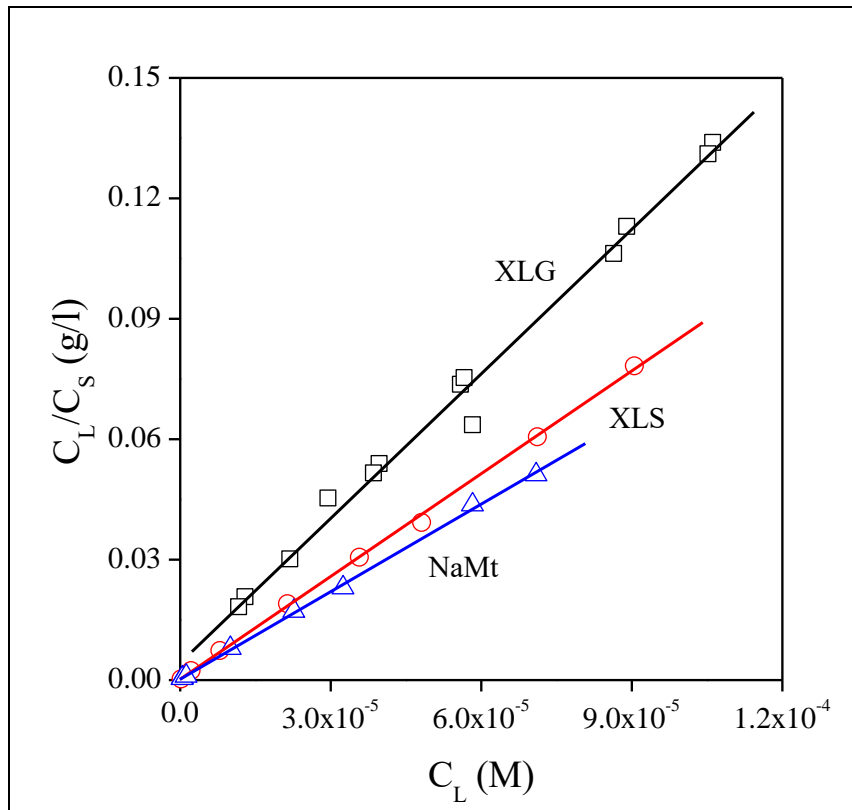
703

704

705 Hegyesi, Fig. 3

706

707



708

709

710

711

712

713

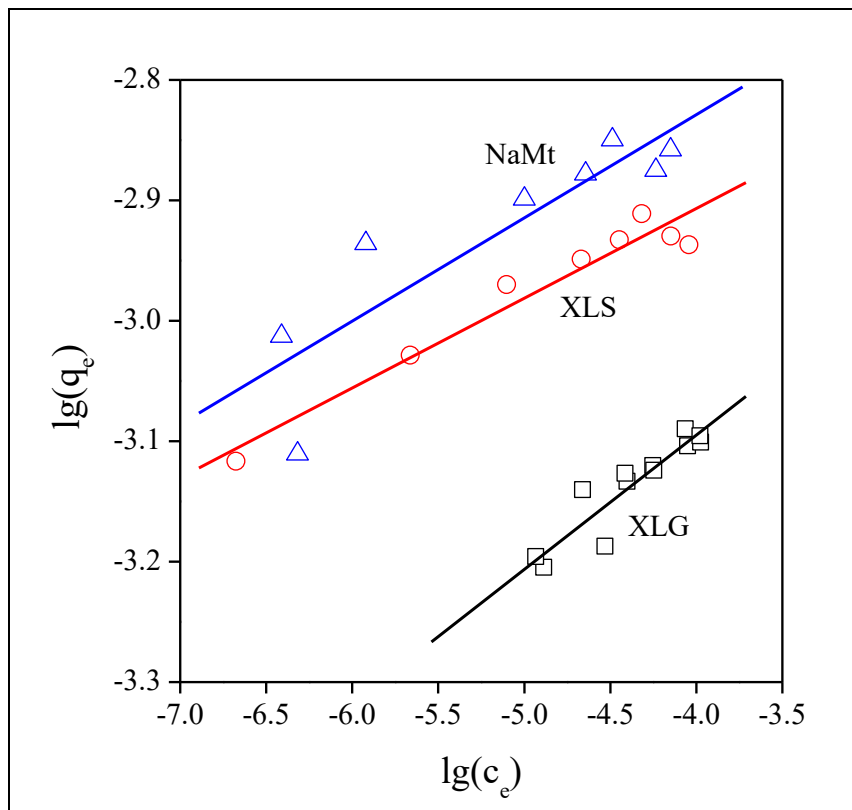
714

715

716 Hegyesi, Fig. 4

717

718



719

720

721

722

723

724

725

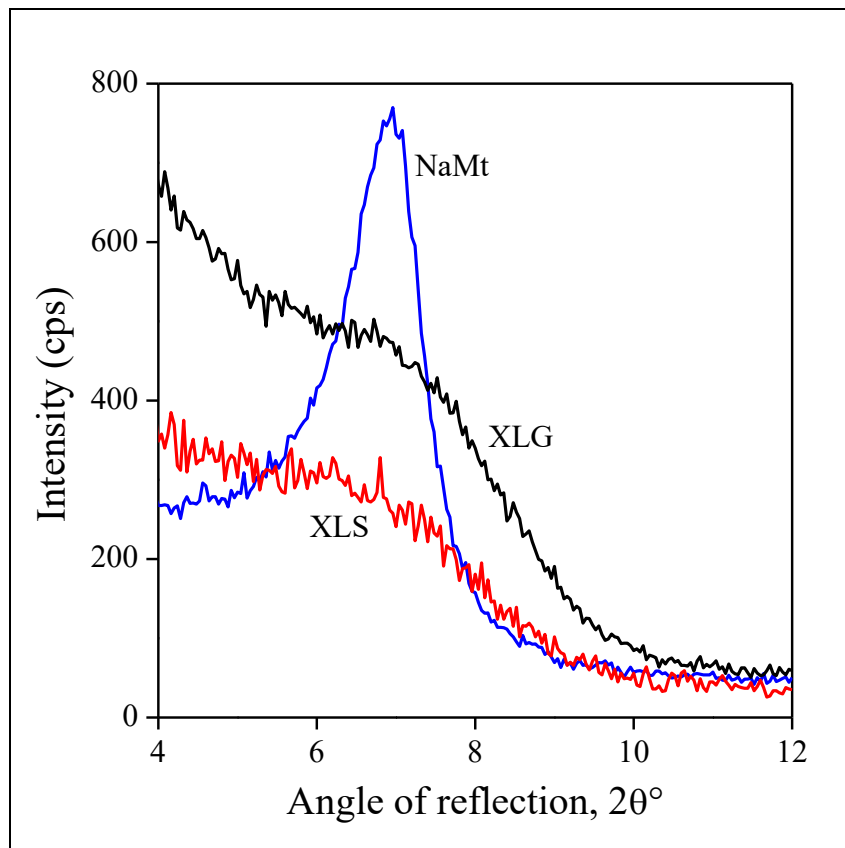
726



727 Hegyesi, Fig. 5

728

729



730

731

732

733

734

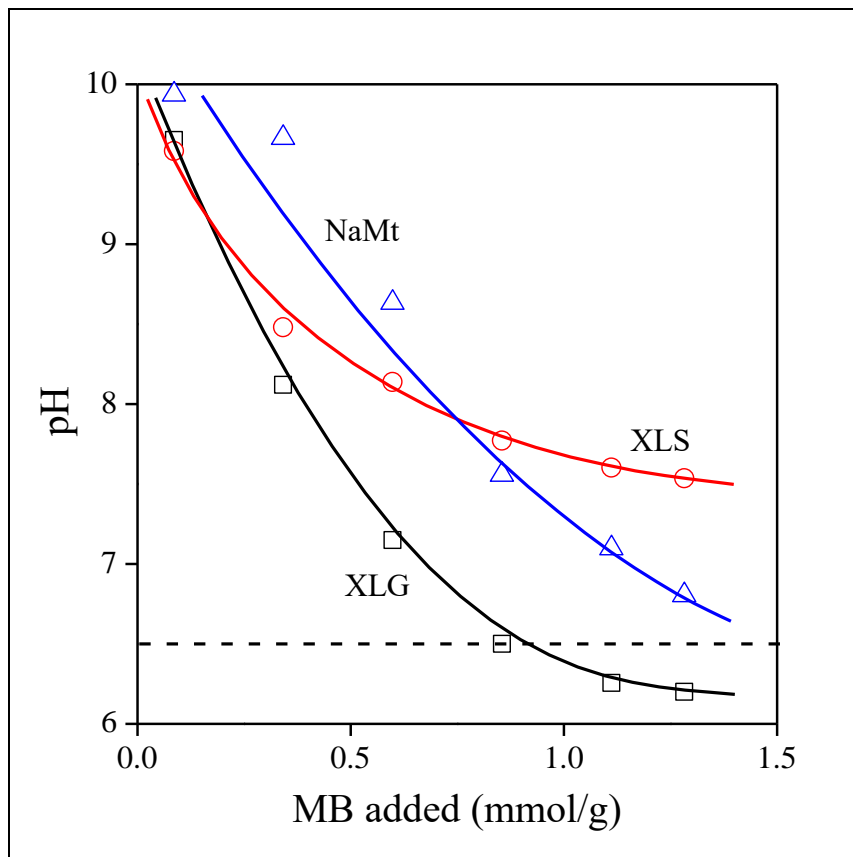
735

736

737 Hegyesi, Fig. 6

738

739



740

741

742

743

744

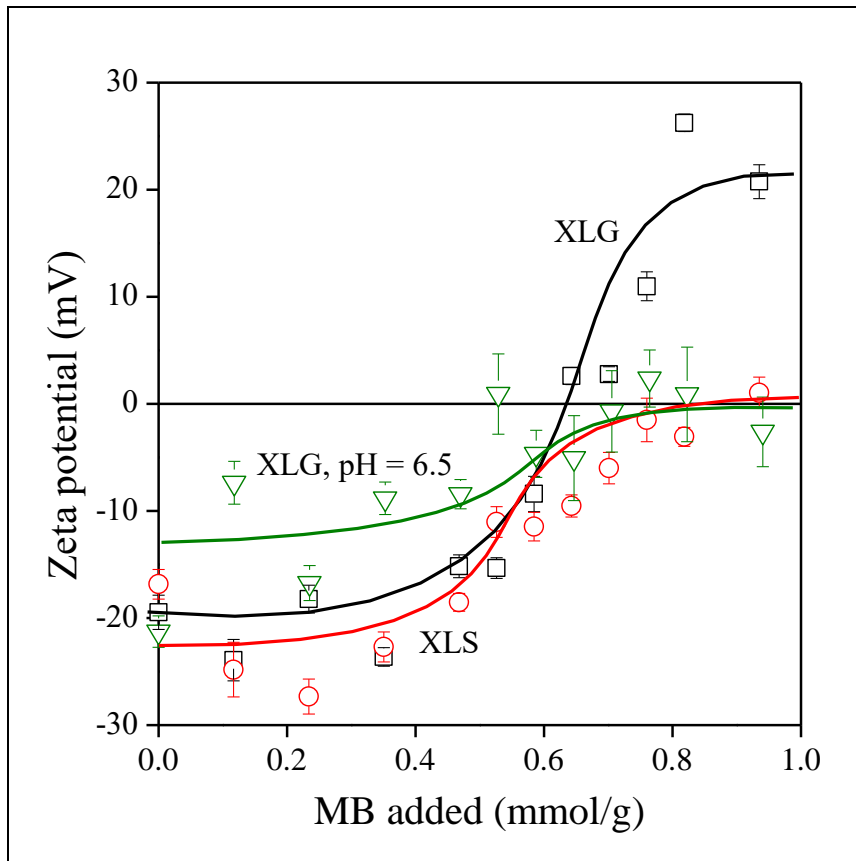
745

746

747 Hegyesi, Fig. 7

748

749



750

751

752

753

754

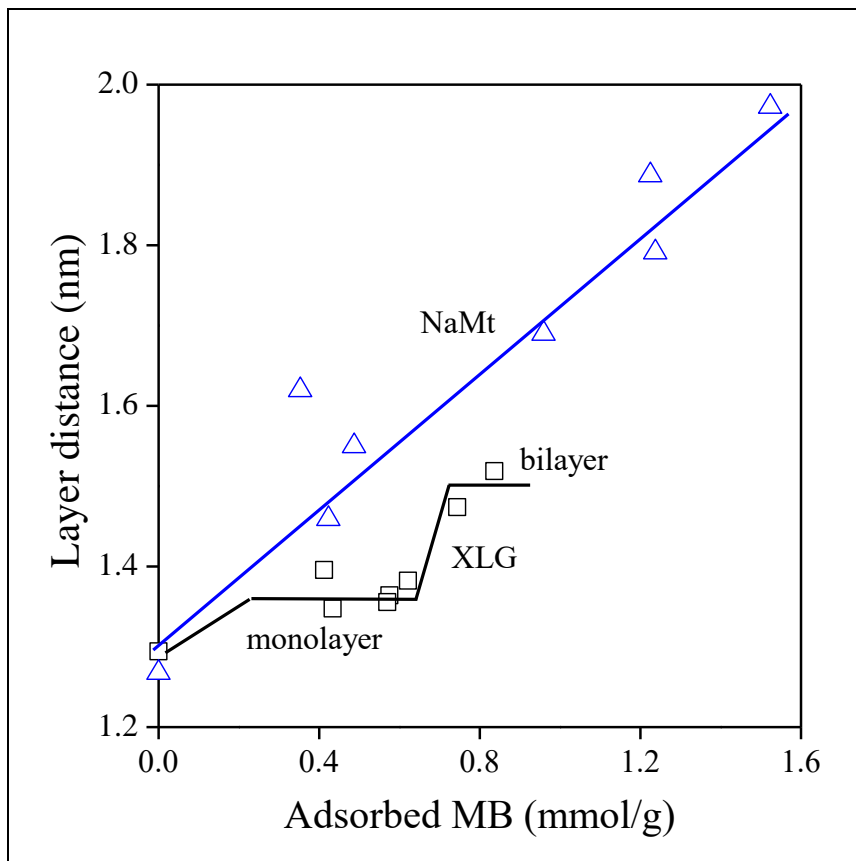
755

756

757 Hegyesi, Fig. 8

758

759



760

761

762

763

764

765